JACS
JOURNAL OF THE AMERICAN CHEMICAL SOCIETY
Article
pubs.acs.org/JACS

Redox Control of the Binding Modes of an Organic Receptor

Marco Frasconi,[†,⊥] Isurika R. Fernando,[†] Yilei Wu,[†,‡] Zhichang Liu,[†] Wei-Guang Liu,[§] Scott M. Dyar,[†,‡] Gokhan Barin,[†,#] Michael R. Wasielewski,[†,‡] William A. Goddard, III,[§,∥] and J. Fraser Stoddart*[,†]

[†]Department of Chemistry, Northwestern University, 2145 Sheridan Road, Evanston, Illinois 60208, United States
[‡]Argonne-Northwestern Solar Energy Research (ANSER) Center, Northwestern University, Evanston, Illinois 60208, United States
[§]Materials and Process Simulation Center, California Institute of Technology, Pasadena, California 91125, United States
[∥]NanoCentury KAIST Institute and Graduate School of EEWS (WCU), Korea Advanced Institute of Science and Technology (KAIST), 373-1 Guseong Dong, Yuseong Gu, Daejeon 305-701, Republic of Korea

Supporting Information

ABSTRACT: The modulation of noncovalent bonding interactions by redox processes is a central theme in the fundamental understanding of biological systems as well as being ripe for exploitation in supramolecular science. In the context of host–guest systems, we demonstrate in this article how the formation of inclusion complexes can be controlled by manipulating the redox potential of a cyclophane. The four-electron reduction of cyclobis(paraquat-*p*-phenylene) to its neutral form results in altering its binding properties while heralding a significant change in its stereoelectronic behavior. Quantum mechanics calculations provide the energetics for the formation of the inclusion complexes between the cyclophane in its various redox states with a variety of guest molecules, ranging from electron-poor to electron-rich. The electron-donating properties displayed by the cyclophane were investigated by probing the interaction of this host with electron-poor guests, and the formation of inclusion complexes was confirmed by single-crystal X-ray diffraction analysis. The dramatic change in the binding mode depending on the redox state of the cyclophane leads to (i) aromatic donor–acceptor interactions in its fully oxidized form and (ii) van der Waals interactions when the cyclophane is fully reduced. These findings lay the foundation for the potential use of this class of cyclophane in various arenas, all the way from molecular electronics to catalysis, by virtue of its electronic properties. The extension of the concept presented herein into the realm of mechanically interlocked molecules will lead to the investigation of novel structures with redox control being expressed over the relative geometries of their components.

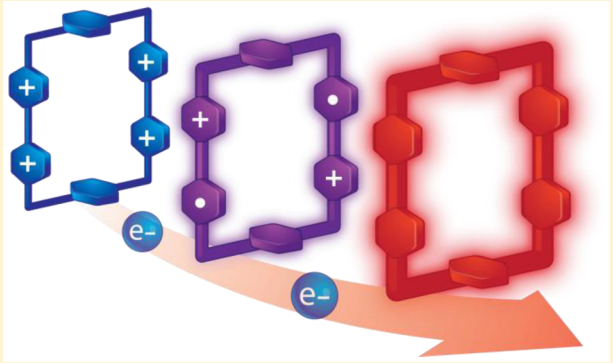

1. INTRODUCTION

The dependence of molecular recognition events on the redox potential of the environment is a fundamental theme in the regulation of biologically relevant processes.[1] Since the binding events between small molecules and certain protein domains—for example, the interaction involving enzyme-cofactor recognition[1]—are mostly electrostatic in nature, the results are particularly sensitive to changes in the charge density distribution within their binding sites. The variety of intermolecular forces governing these recognition phenomena in biological systems has inspired chemists to design and synthesize supramolecular assemblies with precise control of their noncovalent bonding interactions.[2] The investigation of compounds that act as selective molecular receptors with different recognition modes, including hydrophobic forces, hydrogen-bonding, chelation, and aromatic donor–acceptor interactions, and the understanding of the thermodynamic parameters governing the formation of inclusion complexes in a large variety of synthetic macrocycles[3−8] have provided many insights into the nature of noncovalent bonding mechanisms.

The ability to control the formation of stable inclusion complexes has also paved the way for developing a variety of template-directed protocols[9] for the synthesis of mechanically interlocked molecules (MIMs), such as catenanes and rotaxanes. The introduction of bistability into MIMs, by using stimuli responsive host–guest systems, has allowed[10] their actuation, which is accompanied more often than not by large-amplitude motions of their mechanically interlocked components under the action of a stimulus. In this context, the π-electron-poor tetracationic cyclophane, cyclobis(paraquat-*p*-phenylene) ($CBPQT^{4+}$), also known as the "little blue box", has been one of the most extensively investigated[11] building blocks to template the formation of MIMs by harnessing aromatic donor–acceptor interactions. MIMs incorporating $CBPQT^{4+}$ and π-electron-rich recognition sites,[12] such as tetrathiafulvalene (TTF) and 1,5-dioxynaphthalene (DNP), display remarkable properties in the field of mechanostereo-

Received: May 31, 2015
Published: August 3, 2015

DOI: 10.1021/jacs.5b05618
J. Am. Chem. Soc. 2015, 137, 11057−11068

chemistry.[13] Once both of these recognition units are suitably tailored in a catenane or rotaxane, a co-conformational equilibrium where the $CBPQT^{4+}$ ring encircles the better π-donating TTF in preference to the poorer π-donating DNP is established. The reversible co-conformational switching between the two recognition units, induced by cycling the redox state of TTF between its oxidized and reduced forms, has led to the development of a family of molecular switches with tailored thermodynamic and kinetic properties, paving[14] the way for implementation of MIMs as components for molecular electronics.

During the past quarter of century, several variations of the parent $CBPQT^{4+}$ ring have been reported,[15] including various constitutional isomers and larger systems (i) with bitolyl linkers, known[16] as molecular squares (MS^{4+}), or (ii) with extended 1,4-phenylene-bridged bipyridinium units[17] that can be employed as hosts of polycyclic aromatic hydrocarbons (PAHs) on account of their large cavity size. Once it was discovered[18] that the presence of radical-pairing interactions between the diradical dicationic form ($CBPQT^{2(\bullet+)}$) of the little blue box and methyl viologen radical cations ($MV^{\bullet+}$) results in the formation of stable inclusion complexes ($MV^{\bullet+}\subset CBPQT^{2(\bullet+)}$), researchers began to investige[16d,19] the properties of host–guest systems controlled by their redox potential. Template-directed strategies, driven by radical-pairing molecular recognition of 1,10-dialkyl-4,4′-bipyridinium radical cationic ($BIPY^{\bullet+}$) derivatives with $CBPQT^{2(\bullet+)}$ under reductive conditions, have been explored[20,21] as an efficient way to template the formation of mechanical bonds during the synthesis of [2]rotaxanes and [2]catenanes. In the latter case, the inherently tight mechanical bonding of two interlocked $CBPQT^{4+}$ rings led[21a] to the investigation of the solid-state structure of interacting radical species under various oxidation states, showing the existence of mixed-valence species. On account of their unique morphologies and electronic structures, the magnetic properties observed for these species in the solid state afford this class of compounds considerable potential for integration into molecular electronic devices (MEDs).

The fully reduced forms of compounds containing $BIPY^{2+}$ units have also been investigated,[22,23] but only to a small extent in comparison with their radical cationic counterparts. When a methyl viologen derivative in its oxidized form, MV^{2+}, is reduced by two electrons to generate the neutral state, MV, the aromatic rings of the pyridinium units are converted into dihydropyridine rings that display[23] electron-donor properties. This highly reducing species has been employed[24] frequently as a mediator of electron-transfer reactions, including its use[24b] as a catalyst for the reduction of vicinal dibromides in biphasic systems. Recently, the demonstration[25] of the high electronic conductivity of neutral viologen derivatives has made the fully reduced state of this class of compounds particularly attractive as a component in organic MEDs.[26]

The electron-donor properties of neutral BIPY units, in contrast with their electron-deficient dicationic state, have led us to propose that it might be possible to reverse electronically the role of the cyclophane $CBPQT^{4+}$ from being a π-electron-deficient host in the tetracationic form to having an electron-rich cavity in the fully reduced CBPQT state. We envision that developing strategies to control (i) the electronic configuration of synthetic model systems and (ii) the formation of host–guest intramolecular interactions has the potential to uncover new functions associated with more complex processes at the supramolecular level. We argue that the modulation of the

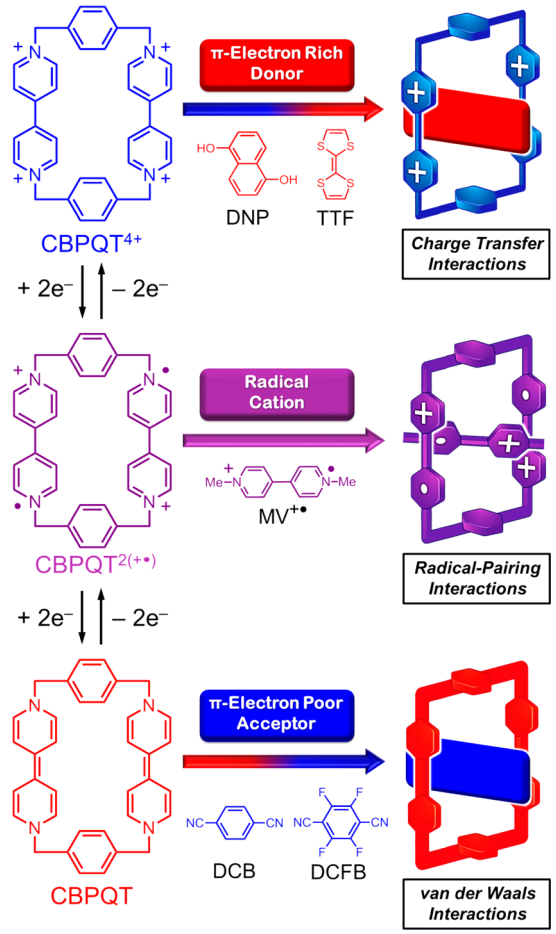

Figure 1. Structural formulas and graphical representations of the redox-controlled modulation of molecular recognition involving charge-transfer (top), radical-pairing (center), and van der Waals (bottom) interactions. These three recognition motifs, involving the tetracationic $CBPQT^{4+}$ (top), the diradical dicationic $CBPQT^{2(\bullet+)}$ (center) and the fully neutral CBPQT (bottom), associated with the three different redox states of the cyclophane, can bind selectively to a large range of substrates, spanning from π-electron-rich to π-electron-poor ones, as well as radical species.

electronic properties of the cyclophane would allow us to explore (Figure 1) a third recognition motif—namely, the neutral CBPQT. Indeed, the cyclophane derived from the complete reduction of the two dicationic $BIPY^{2+}$ units to the electron-rich BIPY motifs can embrace π-electron-poor guests, such as 1,4-dicyanobenzene (DCB) and 1,4-dicyanotetrafluorobenzene (DCFB). The vibrant red color of the solution and the crystals generated from the fully neutral cyclophane leads us to propose calling this electron-rich host the "red box".

In this article, we describe the protocol employed for the preparation of the red box, CBPQT, by four-electron chemical reduction of the blue box, $CBPQT^{4+}$. Moreover, we have characterized the structural and electronic properties of this new receptor in solution using UV–vis, electron paramagnetic resonance (EPR), and NMR spectroscopies. We have also elucidated the structural parameters of the neutral CBPQT and its inclusion complex with DCB in the solid state by using single-crystal X-ray diffraction analysis. Finally, we employed density functional theory (DFT) to provide a quantum mechanical description for the binding energy of the cyclophane units in different redox states, with guests of particular

DOI: 10.1021/jacs.5b05618
J. Am. Chem. Soc. 2015, 137, 11057–11068

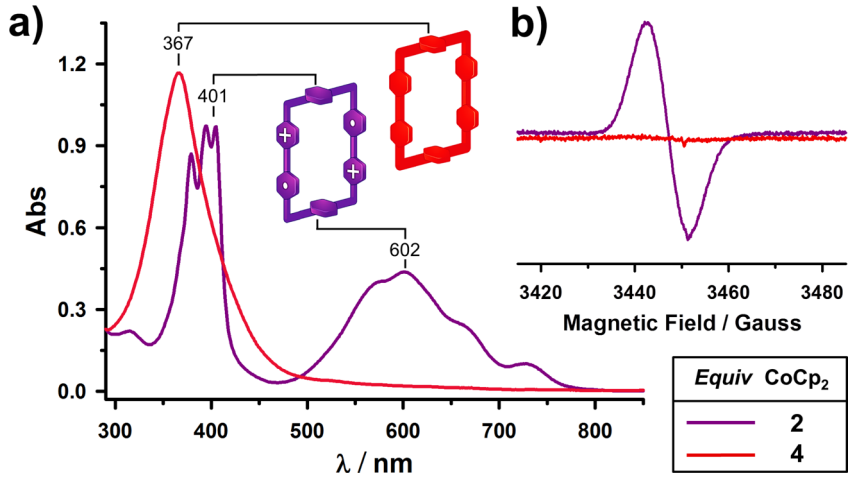

Figure 2. (a) UV−vis absorptions and (b) EPR spectra of diradical dicationic $CBPQT^{2(\bullet+)}$ and neutral CBPQT generated from chemical reduction of a MeCN solution of $CBPQT^{4+}$ (0.08 mM) upon addition of 2 equiv (purple trace) and 4 equiv (red trace) of $CoCp_2$. All spectra were recorded in Ar-purged MeCN solutions at 298 K.

electronic compositions that span the range from π-electron-rich to π-electron-poor compounds.

2. RESULTS AND DISCUSSION

The ability to control the structure of molecules, including the possibility of eliciting substantial changes in their stereoelectronic properties by external stimuli, holds considerable potential for developing functional molecular systems.[27] The existence of three reversible redox states of the multielectron acceptor $CBPQT^{4+}$ means that the stereoelectronic properties of this cyclophane can be switched from complexing with an electron-rich to an electron-poor guest by simply manipulating (Figure 1) its redox chemistry. The $CBPQT^{4+}$ ring undergoes two consecutive reversible two-electron reductions to afford first the diradical dicationic $CBPQT^{2(\bullet+)}$ and then second, the fully reduced CBPQT ring. These reductions occur at redox potentials of −328 and −753 mV, respectively, as measured in MeCN solution versus a SCE reference.[18] We used UV−vis and EPR spectroscopies to probe the physicochemical properties of the cyclophane in its different oxidation states, generated by titrating the strong chemical reductant cobaltocene ($CoCp_2$) into a MeCN solution of the tetracationic $CBPQT^{4+}$ under an Ar atmosphere. The use of $CoCp_2$ as a chemical reducing agent in homogeneous phase has several advantages, including (i) affording a significant driving force for the reduction of $BIPY^{2+}$ derivatives into their neutral states, thanks to its sufficiently negative reduction potential,[28] and (ii) providing precise control over the number of equivalents of the reducing agent per equivalent of $CBPQT^{4+}$. Upon stepwise addition of the reductant, we detected a gradual increase of the diradical dicationic $CBPQT^{2(\bullet+)}$ (Figure 2a and Supporting Information, Figure S10) as shown by the emergence in the UV−vis spectrum of two sets of absorption bands, centered on 401 and 602 nm, indicating the distinctive feature of vibronic coupling. The increase in intensity of the EPR signal upon addition of $CoCp_2$ up to 2 equiv (Figures 2b and S12), which is proportional to the height of the visible absorption band at 602 nm, provides evidence for a high-spin exchange regime between the unpaired electrons in the $BIPY^{\bullet+}$ units of the cyclophane. This observation is also consistent with the absence of the hyperfine structure that is usually observed in radical cationic species of non-interactive viologen derivatives (see Figure S13) and also with the quantum mechanical calculations.

In excess of 2 equiv of reductant, we observe (i) a decrease in intensity of these absorption bands, which is associated with the diradical dication and (ii) the concomitant increase in intensity of a new band at 367 nm in the UV−vis spectrum, indicating formation of doubly reduced BIPY units within the cyclophane, in line with the spectra reported[22,23] for other neutral dihydrobipyridyl compounds. Evidence for the generation of neutral CBPQT in quantitative yield upon addition of 4 equiv of reductant was provided by (i) the red color of the solution with an intense absorption band at 367 nm, along with (ii) the disappearance of the EPR signal, indicating (iii) the absence of radical character in the fully reduced form.

In order to probe in more detail the physicochemical properties of fully reduced CBPQT and investigate the formation of inclusion complexes with a series of guests, as well as its potential use in the templated-directed synthesis of MIMs, we need to develop a protocol for its preparation and quantitative isolation. One possible approach to the isolation of the neutral species from its charged counterparts resides in performing the redox chemistry in a heterogeneous two-phase system composed of an aqueous solution and PhMe. The design of an efficient method for the reduction of $CBPQT^{4+}$, followed by extraction of the neutral species, takes advantage of the dependence of the cyclophane solubility on its redox states. Thus, the chloride salt of the cyclophane, CBPQT·4Cl, is soluble only in the aqueous phase while the diradical dication is slightly soluble in both phases: in contrast the neutral CBPQT is soluble only in the organic layer. We prepared a stable colorless solution of $CBPQT^{4+}$ in the aqueous alkaline (pH 9.0) solution of the biphasic system[29] under an Ar atmosphere. The subsequent addition of a small excess (6 equiv) of sodium dithionite results in the aqueous phase turning dark blue-purple, followed by a change in the color of the PhMe layer, first of all to yellow and, after a few minutes, to an intense red color. The UV−vis absorption spectrum of the PhMe phase displays (Figure 3a) a band with a maximum at 365 nm, corresponding to the absorption of fully reduced BIPY units in the CBPQT. We also observed an increase in the intensity of the color of the organic phase with a rise in the concentration of $CBPQT^{4+}$ in the aqueous layer, ranging from 0.1 to 5 mM.

DOI: 10.1021/jacs.5b05618
J. Am. Chem. Soc. 2015, 137, 11057−11068

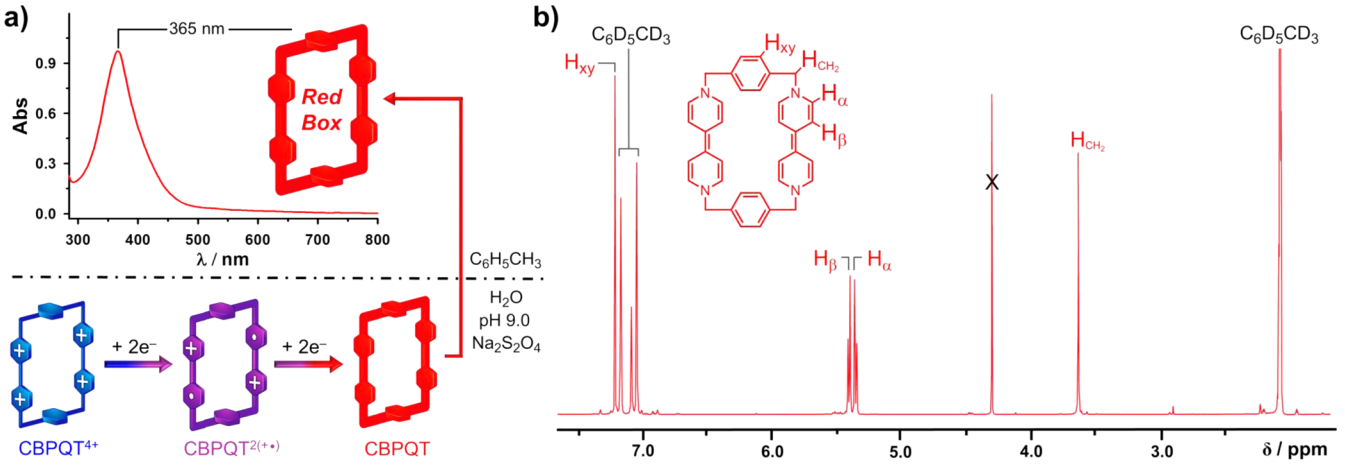

Figure 3. (a) UV−vis absorption spectrum of the neutral CBPQT in PhMe, obtained by chemical reduction of $CBPQT^{4+}$ with $Na_2S_2O_4$ followed by extraction from a heterogeneous two-phase system composed of PhMe and an alkaline (pH 9.0) aqueous layer. (b) ^1H NMR spectra (500 MHz, $C_6D_5CD_3$, 298 K) of a solution of neutral CBPQT transferred to $C_6D_5CD_3$ by extraction from the biphasic system.

The absence of the characteristic absorption bands of the diradical dication in the UV−vis spectra of the organic phase is an indication that direct reduction of $CBPQT^{2(\bullet+)}$ to the neutral CBPQT state takes place in the aqueous phase, followed by its extraction into the PhMe layer. We cannot exclude the possibility that a small fraction of the radical cationic $CBPQT^{2(\bullet+)}$ may be extracted from the aqueous phase into the organic layer, due to the slight solubility of the radical cationic ring in PhMe. On the other hand, a fast disproportionation[22,24b] is expected to take place to this small fraction of $CBPQT^{2(\bullet+)}$ in the organic layer. The disproportionation of $CBPQT^{2(\bullet+)}$ results in the formation of two products—the tetracationic $CBPQT^{4+}$ and the neutral CBPQT—exhibiting quite different solubilities. In the two-phase system, the extraction of the $CBPQT^{4+}$ out of the organic layer into the aqueous phase drives the disproportionation reaction to completion. The combination of (i) the direct reduction of $CBPQT^{4+}$ to its neutral form and (ii) the disproportionation of the intermediate radical cationic $CBPQT^{2(\bullet+)}$ to its neutral and tetracationic forms leads to the efficient production of the neutral CBPQT in the PhMe phase in a yield estimated[30] to be close to 90%. While a PhMe solution of the neutral CBPQT is stable in air for a few minutes, a solution of the $CBPQT^{2(\bullet+)}$ in MeCN undergoes oxidation much more readily, indicating that the bisradical dication is much lower in stability to oxygen than is the neutral cyclophane.

The diamagnetic nature of the ring structure in the fully reduced cyclophane, as revealed by EPR spectroscopy, makes feasible the solution-state characterization (Figures 3b and S2−S4) of neutral CBPQT by ^1H and ^{13}C NMR spectroscopies. A red CBPQT solution was obtained readily by extracting CBPQT from a biphasic system using $C_6D_5CD_3$ as the organic layer under an Ar atmosphere. The presence of a single species in the $C_6D_5CD_3$ phase was confirmed by diffusion-ordered ^1H NMR spectroscopy, which reveals (Figure S3) the presence of a single band corresponding to a diffusion coefficient of 1.7×10^{-10} m^2 s^{-1}. The addition of two electrons to each of the $BIPY^{2+}$ units of the cyclophane has a dramatic effect on the resonances[31] (Figure 3b) of the protons, whose assignments were confirmed by 2D NMR experiments (Figures S5 and S6). The peaks corresponding to H_α and H_β on the BIPY unit can be identified at around 5.32 and 5.36 ppm, respectively, revealing much less aromatic character with respect to the protons in positions α and β to the nitrogens on the $BIPY^{2+}$ units which resonate much further downfield.[32] This change in the ^1H NMR spectrum of the neutral CBPQT, in comparison with the tetracationic cyclophane $CBPQT^{4+}$, is accompanied by upfield shifts to 3.62 ppm of the resonances associated with the methylene group protons. These upfield shifts observed for the protons from the BIPY units that constitute the neutral cyclophane are a direct result of the loss of aromaticity by the BIPY units in their fully reduced states. The conversion to a nonaromatic planar structure is supported by the ^{13}C NMR spectrum (Figure S4) that reveals shifts in the resonances of the α and β carbons to δ values characteristic of polyene-like structures.[22]

The solid-state structure of the neutral CBPQT ring was obtained by X-ray crystallographic analysis[33] of the deep red crystals. Single crystals of CBPQT were grown at 0 °C by slow vapor diffusion of *n*-hexane into a 0.5 mM MeCN solution of $CBPQT^{4+}$, following reduction to the neutral redox state with 4 equiv of $CoCp_2$ under an Ar atmosphere. Red crystals of the fully reduced cyclophane, suitable for X-ray diffraction analysis, were also observed to grow spontaneously upon four-electron reduction of a 5 mM solution of $CBPQT^{4+}$ in MeCN at room temperature. The X-ray structural analysis[34] shows (Figure 4) that the solid-state structure of the neutral CBPQT adopts a parallelogram-like conformation, despite the relatively high rigidity of the box-like molecule, with the BIPY units occupying the longer sides. In comparison with the blue rectangular box-like conformation of $CBPQT^{4+}$, the "corner" angles increase (Figure 4b) from 108° to 113° for the red neutral CBPQT. The separation between the CBPQT molecules (Figure S16) precludes any interactions between the cyclophanes in their long-range packing order and excludes the possibility of conformational distortion arising from lattice effects. The dimension of the cavity, measured as a centroid-to-centroid distance between the planes of the two BIPY units of the ring is 6.99 Å, similar to the values reported[32] for the tetracationic, as well as the diradical dicationic, oxidation states of the cyclophane. The absence of counterions in the unit cell confirms the neutral nature of the red box. The lack of free radicals was established (Figure S14) by solid-state CW EPR spectroscopy performed on single crystals of CBPQT. Analysis (Table 1) of the bond lengths and torsional angles of the BIPY units provides a quantitative measurement of the redox state of

DOI: 10.1021/jacs.5b05618
J. Am. Chem. Soc. 2015, 137, 11057−11068

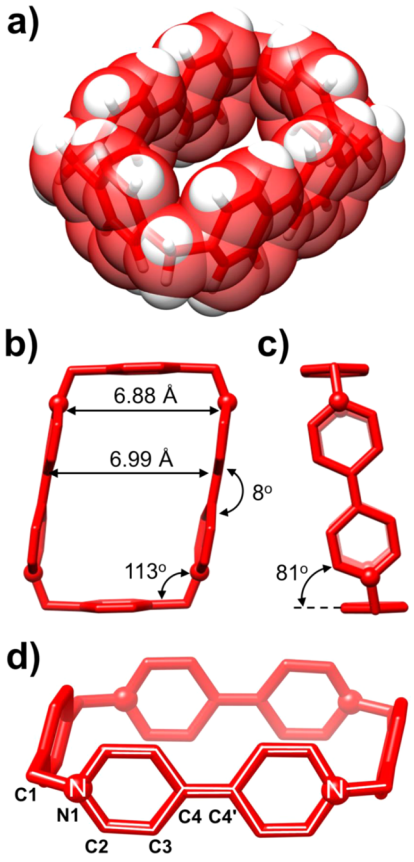

Figure 4. Solid-state structure of the neutral CBPQT obtained from single-crystal X-ray crystallography. (a) Perspective view of the CBPQT ring as a tubular representation with the corresponding semitransparent space-filling representation superimposed upon it. (b,c) Plan and side-on views of the CBPQT ring as a tubular representation showing distances and angles displaying the ring's geometry. (d) Perspective view in which the localized double and single bonds are superimposed on a tubular representation. The corresponding bond lengths and angles are reported in Table 1. The solvent molecules have been omitted for the sake of clarity.

the BIPY units. The torsional angle measured around the C4−C4′ bond of the BIPY unit in the CBPQT is 8°, indicating the increased double-bond character of the C4−C4′ bonds. The central bond distance is also known[23] to correlate well with the redox state, showing a marked deviation from the length of the single bond in the $BIPY^{2+}$ to the double bond character for the neutral BIPY units. In the case of the CBPQT, the C4−C4′ bond length is 1.37 Å, corresponding to a double bond. Localized double bonds, with lengths of 1.32 Å, are also evident for the C2−C3 bonds. A different situation is observed for the C3−C4 bonds which, with a distance of 1.46 Å, can be consider to be a localized single bond between sp^2 hybridized atoms if compared with 1.45 Å for the central bond of butadiene. These alternating bond lengths, which are similar to those reported by Kochi[23] for the fully reduced MV, confirm the successful conversion of the cyclophane to its neutral state.

The unique stereoelectronic properties that accompany the fully reduced BIPY units—such as their relatively high solid-state electronic conductivity—within the molecular framework of the cyclophane opens up possibilities for its future exploitation as an active component in MEDs. In essence, understanding the behavior of this host as an effective isostructural dopant for particular guests, that may induce specific electronic properties out of a large range of possibilities, offers an alternative supramolecular strategy for realizing new organic electronic materials. We anticipate that a minimal change in geometrical relaxation during the hole transfer of neutral molecules is highly desirable[35] in order to attain high solid-state conductivity in MEDs. Indeed, the small changes observed in the bond lengths and bond order between the neutral BIPY and the radical cationic $BIPY^{\bullet+}$—the latter being the relevant species for conduction by neutral BIPY in the solid state[25,35]—renders this an attractive unit to be incorporated into devices that take advantage of its solid-state conductivity properties. With the incentive of understanding the conformational changes and the properties associated with different redox states of supramolecular assemblies, we investigated the solid-state superstructure of an assembly comprised of two redox states of the CBPQT ring—namely, the neutral and the diradical dicationic forms. Mixed redox systems based on viologen derivatives that have been investigated[36] in solution and in the solid state reveal a high degree of electronic coupling between the dication and the radical cation. Despite the rapid disproportionation that occurs in the case of the radical cationic

Table 1. Selected Bond Distances and Torsional Angles for Solid-State Structures[a] and DFT-Calculated Structures[b] of BIPY Derivatives under Different Oxidation States

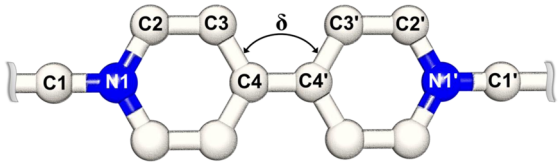

	bond lengths/Å					
BIPY derivative	C1−N1	N1−C2	C2−C3	C3−C4	C4−C4′	torsional angle δ/°
$CBPQT^{4+}$ [c]	1.49 (1.50)	1.34 (1.35)	1.38 (1.38)	1.39 (1.40)	1.48 (1.48)	21 (32)
$CBPQT^{2(\bullet+)}$ [d]	1.49 (1.48)	1.35 (1.37)	1.37 (1.36)	1.43 (1.43)	1.43 (1.43)	2.6 (2.3)
CBPQT	1.47 (1.46)	1.39 (1.39)	1.32 (1.35)	1.46 (1.46)	1.37 (1.38)	8.1 (2.5)
MV[e]	1.45 (1.45)	1.38 (1.39)	1.33 (1.35)	1.46 (1.46)	1.36 (1.38)	6.0 (0.4)
MS	1.44 (1.46)	1.39 (1.39)	1.31 (1.35)	1.48 (1.46)	1.38 (1.38)	1.5 (1.3)
DCB⊂CBPQT	1.46 (1.46)	1.39 (1.39)	1.34 (1.45)	1.45 (1.45)	1.38 (1.38)	3.5 (1.8)

[a]Data obtained from X-ray crystallographic analysis. [b]In parentheses, data obtained from DFT calculation at the M06[1]/6-311++G**//M06/6-31G* level. [c]Crystal data for CBPQT·4PF_6 from ref 32. [d]Crystal data for CBPQT·2PF_6 from ref 18b. [e]Crystal data for MV from ref 23.

DOI: 10.1021/jacs.5b05618
J. Am. Chem. Soc. 2015, 137, 11057−11068

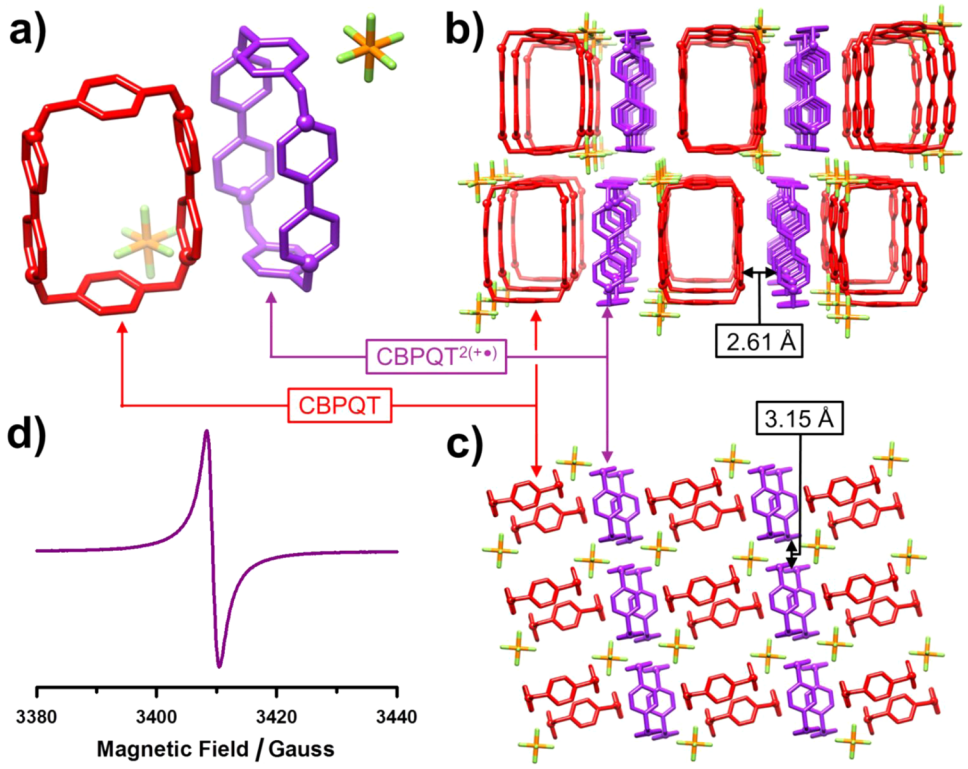

Figure 5. Tubular representations of the solid-state superstructures of a mixed oxidation state (CBPQT)(CBPQT·2PF_6). (a) Plan and side-on views of the unit cell revealing the presence of the neutral CBPQT (red box) and the diradical dicationic CBPQT$^{2(\bullet+)}$ (purple box) surrounded by two PF_6^- counterions. (b) The solid-state packing of (CBPQT)(CBPQT·2PF_6), in plan and side-on views, revealing the packing of the CBPQT and CBPQT$^{2(\bullet+)}$ redox states and the relative positions of the counterions. (c) Top view of the solid-state packing, showing the stack of BIPY$^{\bullet+}$ units in the CBPQT$^{2(\bullet+)}$ rings along the *a*-axis. The face-to-face distance between the BIPY$^{\bullet+}$ components is 3.15 Å. (d) Solid-state CW EPR spectrum of single crystals of (CBPQT)(CBPQT·2PF_6), demonstrating the presence of free radicals in the solid-state structure in accordance with the observation of two counterions in the solid-state superstructure.

BIPY$^{\bullet+}$, we have been able to grow single crystals from an equimolar mixture of CBPQT$^{2(\bullet+)}$ and CBPQT obtained from chemical reduction by using, respectively, 2 and 4 equiv of $CoCp_2$ in MeCN, followed by the slow vapor diffusion of iPr_2O at 0 °C under an Ar atmosphere. The resulting purple-black crystals are clearly distinct from the vibrant green color of the solution that results from an equimolar mixture of the blue CBPQT$^{2(\bullet+)}$ and red CBPQT solutions. The unit cell, as determined by X-ray crystallography,[37] is comprised (Figure 5a) of two independent cyclophanes in which the plane of one ring, defined by its four N atoms, is orthogonal to the plane of the other ring: they are surrounded by a total of two PF_6^- counterions. The extended superstructure reveals two different segregated stacks of CBPQT molecules, separated by PF_6^- anions (Figure 5b) and composed of (i) a one-dimensional superstructure with the red cyclophane forming a continuous channel and (ii) an infinite stacking of the purple cyclophane maintained by interactions between their BIPY subunits. The nature of the two different layers made of cyclophanes in different redox states has been elucidated by their structural characteristics and the presence of counterions surrounding each ring.[38] The layer of cyclophanes with the BIPY units face-to-face are diradical dicationic CBPQT$^{2(\bullet+)}$ rings as deduced from the bond order of the BIPY units, including the radical cationic character (1.42 Å) of the C4−C4′ bond. The packing of the diradical dicationic CBPQT$^{2(\bullet+)}$ rings comprises (Figure 5c) a one-dimensional stack with a centroid-to-centroid separation of 3.15 Å between the BIPY$^{\bullet+}$ units of the adjacent CBPQT$^{2(\bullet+)}$ rings, indicating the presence of radical-pairing interactions between their BIPY$^{\bullet+}$ components, stabilizing their superstructure. The existence of the diradical dicationic CBPQT$^{2(\bullet+)}$ in the mixed redox-state crystal was also revealed by solid-state EPR spectroscopy. An isotropic EPR spectrum (Figure 5d) was obtained on some single crystals with *g* factors close to the ones reported for radical cationic MV$^{\bullet+}$ in the solid state. By simply manipulating the redox chemistry of the cyclophane, we have demonstrated the formation of an ordered system comprised of stacks of diradical dicationic CBPQT$^{2(\bullet+)}$ units segregated between neutral layers of CBPQT rings.

In order to explore the unique properties of neutral BIPY in differently confined environments and to shed more understanding on the redox-controlled organization of supramolecular assemblies, we have investigated the effect of neutral BIPY units on the packing of other cyclophanes. In particular, we have examined the possibility of obtaining structural information on the fully reduced BIPY units in larger cyclophanes, such as the organic molecular square, MS^{4+}, which is comprised of bitolyl units linking bipyridinium rings. The first two-electron uptake for the MS^{4+} produces the diradical dicationic MS$^{2(\bullet+)}$ and the second two-electron transfer leads (Figure 6a) to the fully reduced neutral form, MS. The UV−vis absorption spectra, measured during the course of a redox titration of a DMF solution[39] of MS^{4+} results (Figure S11), on addition of 2 equiv of $CoCp_2$, in an absorption band appearing at 610 nm that is associated with the formation of the radical cationic BIPY$^{\bullet+}$. Conversion to the fully reduced MS, which was achieved quantitatively on the addition of 4 equiv of $CoCp_2$, results in the complete disappearance of the

DOI: 10.1021/jacs.5b05618
J. Am. Chem. Soc. 2015, 137, 11057−11068

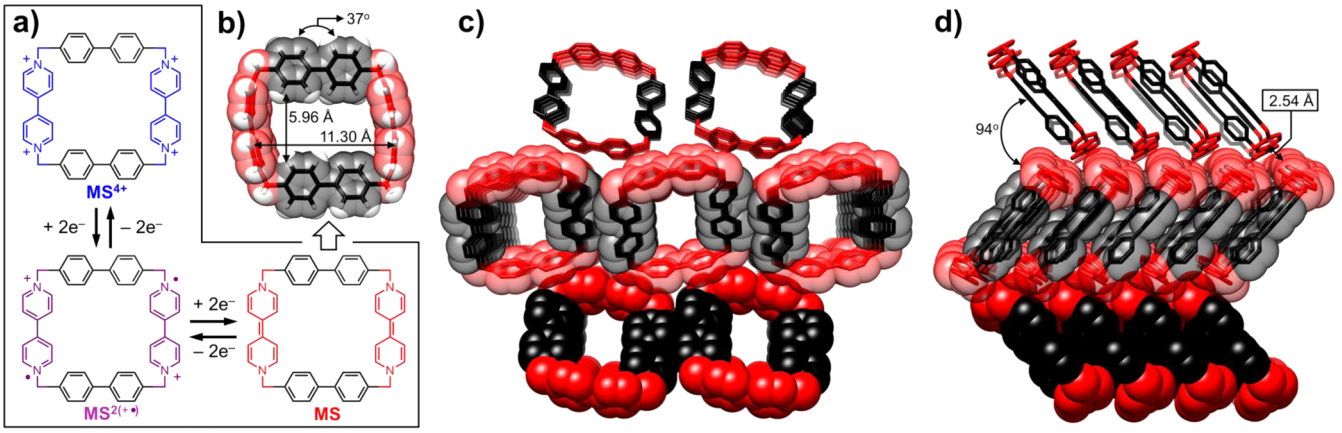

Figure 6. (a) Structural formulas illustrating the reversible pair of two-electron reductions of MS^{4+}, leading to the formation of the diradical dicationic $MS^{2(\bullet+)}$ and subsequently the neutral MS. (b) Space-filling overlying a tubular representation of the solid-state structure in plain view of the neutral MS obtained from single crystal X-ray crystallography. The rotation of the bitolyl linkers results in the decrease in the width of the cavity to 5.96 Å. In common with the neutral CBPQT, the BIPY units of the neutral MS display alternation of their double and single bonds. (c) Plan view along the *a*-axis of the long-range packing order of MS, using a tubular (top) and a space filling (bottom) representation, revealing the porous nature of the superstructure defined by the empty square macrocycles. (d) Side-on view of the solid-state structure of MS, represented in tubular (top) and space filling (bottom) formats, showing the packing of the neutral rings stabilized by [C−H···π] interactions (2.54 Å).

absorption band of the radical cationic species and the emergence of an absorption band at 380 nm, characteristic of the neutral species. We have also investigated the structural changes which occur upon reduction of MS^{4+} to its neutral form by X-ray crystallography. Single crystals were grown at 0 °C under an Ar atmosphere by slow vapor diffusion of iPr_2O from a 2 mM DMF solution of $MS{\cdot}4PF_6$ containing a slight excess of $CoCp_2$ (5.0 equiv) in order to ensure the complete reduction of the molecular square to the neutral state. This neutral state of MS in the X-ray crystal structure[40] (Figure 6b) is confirmed by the bond length analysis (Table 1) of the BIPY units, which alternate between localized double and single bonds, as well as the absence of PF_6^- counterions in the unit cell. The reduction of the MS^{4+} to its neutral state is accompanied by significant changes in the solid-state structure of the molecular square compared with those observed for the tetracationic[16b] and diradical dicationic forms.[16d] The most noticeable change is in the angle defined by the plane of the aromatic rings of the bitolyl linker with respect to the plane of the molecular square. The reduction to the neutral BIPY units induces a rotation of almost 90° in the bitolyl linkers around the axis defined by the two methylene carbon atoms, such that the phenylene rings point inside the cavity of the molecular square. The rotation of the bitolyl linkers leads to a dramatic decrease in the width of the cavity, defined by the distance between the planes of the phenylene rings, from 11.0 Å for the MS^{4+} to 5.94 Å in the case of the neutral MS. There is a torsional angle of 37° between the phenylene rings of the bitolyl linkers.

A second key influence of the redox state on the structural properties of the cyclophane is observed in the extended solid-state superstructure. The packing of neutral MS molecules reveals (Figure 6c) an arrangement of the rings in which the cavities define continuous porous channels. By contrast, the rings of the neutral CBPQT exist in the solid-state structure as separate entities. Examination of the superstructure of the fully reduced MS shows (Figure 6d) that noncovalent bonding interactions between the neutral BIPY units help to sustain the packing of the MS rings. We attribute the stabilization of the channels to the formation of [C−H···π] interactions with a mean distance of 2.54 Å between protons on the BIPY units in one sheet with the centroid of the BIPY ring in another channel. We note here that the bitolyl linkers, despite their apparent face-to-face arrangement, do not participate in the stabilization of the superstructure. The organization of these rigid neutral cyclophanes in the solid state opens up the possibility of using single crystals of these cyclophanes as materials for electronic applications. Finally, the ability of redox chemistry to activate selectively the rotation of the bitolyl linkers, resulting in the "breathing" of the cavity of the cyclophane between an open and a closed state, demonstrates a fundamental relationship between structure and redox properties that will enable us to explore more intricate phenomena at the supramolecular level.

The fact that the electronic properties of $CBPQT^{4+}$ are dramatically altered upon its reduction to the neutral form—resulting in a completely new host, the red box CBPQT—should, in turn, also change significantly its preference for guests. Thus, we envision that the electron-rich cavity of the CBPQT will provide an ideal fit to accommodate electron-poor guests, opening up the possibility of using the redox potential to modulate the binding modes of the host toward a myriad of guest molecules, ranging from the more classical π-electron-rich guests to a spectrum of π-electron-poor guests. In order to probe the guest-binding properties of the neutral CBPQT, we investigated 1,4-dicyanobenzene (DCB) and 1,4-dicyanotetrafluorobenzene (DCFB) as π-electron-poor guests to determine whether they can be embraced, based on stereoelectronic considerations, by the neutral CBPQT to undergo formation of stable inclusion complexes.

To test this hypothesis, we employed ^{1}H NMR spectroscopy to evaluate the formation of the inclusion complexes between the CBPQT and DCB or DCFB guests. Our initial experiments, carried out in $C_6D_5CD_3$ solutions containing neutral CBPQT, which was separated from the biphasic system, showed only a small upfield shift in the resonance associated with the α protons of the CBPQT unit, along with the signals corresponding to the methylene protons, upon addition of the guest.[41] The differences between the chemical shifts of the α protons of the CBPQT in the absence and in the presence of

DOI: 10.1021/jacs.5b05618
J. Am. Chem. Soc. 2015, 137, 11057−11068

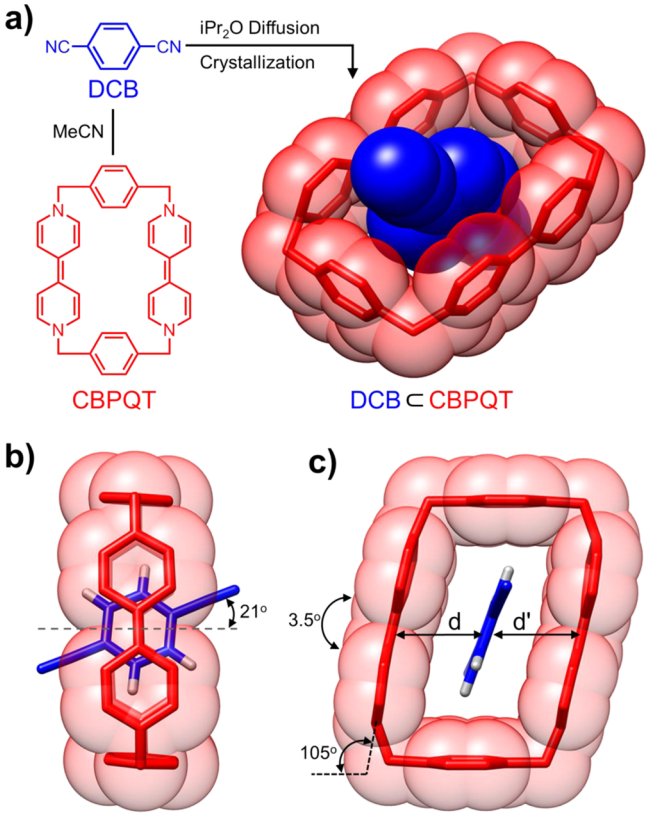

Figure 7. Solid-state superstructures of the complex of CBPQT with 1,4-dicyanobenzene as the substrate. (a) Perspective view of the inclusion complex with DCB, displayed with the CBPQT ring in semitransparent space-filling format, superimposed upon a tubular representation, and with the guest in space-filling format, highlighting the degree of envelopment of DCB by CBPQT. (b) Side-on view using a tubular/space-filling representation of the solid-state superstructure of DCB⊂CBPQT showing the angle subtended by the axis of DCB, defined by its C≡N bonds, with the axis orthogonal to the plane of the CBPQT ring defined by the four N atoms of the ring. (c) Plan view employing a tubular/space-filling representation of the 1:1 inclusion complex with average distances between the DCB and the BIPY walls of the CBPQT ring of 3.47 Å (d) and 3.45 Å (d'), measured from the centroid of the aromatic ring of DCB to the center of the C4−C4′ bond of the BIPY unit.

DCB and DCFB were respectively 0.005 and 0.012 ppm (Figure S9). These results suggest that the binding of DCB and DCFB within the cavity of the CBPQT are quite weak in $C_6D_5CD_3$ solution.[42] The lack of a charge-transfer (CT) band in the UV−vis absorption spectrum of a 1:1 mixture of CBPQT and DCB or DCFB indicates that the affinity between the CBPQT and thus π-electron-poor guests does not arise primarily from CT interactions, an observation that explains the modest binding constants. We speculate that the formation of the inclusion complexes, involving neutral CBPQT, is a consequence of favorable electrostatic interactions,[43] an observation which is confirmed by the quantum mechanical description of the binding in the complexes.

Clear evidence for the ability of the neutral CBPQT to form 1:1 inclusion complexes with π-electron-poor guests was obtained by X-ray crystallography. Despite the weak association, we were able to obtain red single crystals at 4 °C by slow vapor diffusion of n-hexane into a MeCN solution of CBPQT containing DCB under Ar. The X-ray structural analysis[44] reveals (Figure 7a) that the DCB guest is located at a centrosymmetric site inside the cavity of the neutral CBPQT host, sharing the same space group observed for a single crystal of the free CBPQT host. The axis defined by the C≡N groups of the DCB, which protrudes above and below the rims of the host, subtends (Figure 7b) an angle of 21° with the axis orthogonal to the plane, defined by the four N atoms of the ring. This deviation from the orthogonality permits an efficient orbital overlap between the aromatic ring of the guest and the two BIPY units in the CBPQT host. The distances between the guest and the two BIPY walls of the CBPQT, measured (Figure 7c) from the centroid of the aromatic ring of DCB to the central double bond of the BIPY units, are 3.45 and 3.47 Å, both distances typical of π-stacking interactions. Two of the aromatic protons on the DCB guest are also engaged in [C−H···π] interactions with the phenylene units of the CBPQT host and presumably contribute to the overall stability of the complex. The solid-state superstructure indicates that the dimensions and the conformation of the CBPQT are unchanged on complexation with the guest. A subtle decrease of the torsional twist of the BIPY unit around the C4−C4′ bond to 3.5° could be a result of the accommodation of the π-electron-poor guest within its π-electron-rich cavity.

Density functional theory at the M06[1]/6-311++G**//M06/6-31G* level with the Poisson−Boltzmann solvation model[45] of MeCN was used to calculate the enthalpies of complexation that govern the binding of guests with the cyclophane in its different oxidation states. The concept of reversing the binding mode of the cyclophane by altering its redox state becomes more evident (Figure 8 and Table S1) by comparing the predicted complexation enthalpies of guests comprising electron-rich and electron-poor molecules, with the cyclophane in redox states ranging all the way from tetracationic to neutral. In the context of this research, the complexation enthalpy is defined as the energy it takes for a guest to replace two MeCN molecules originally sitting in the cavity of the cyclophane—representing the free cyclophane in MeCN solvent—to form a 1:1 inclusion complex.

We uncovered a general trend associated with the charge on the CBPQT and the electron-richness of the guests. This trend

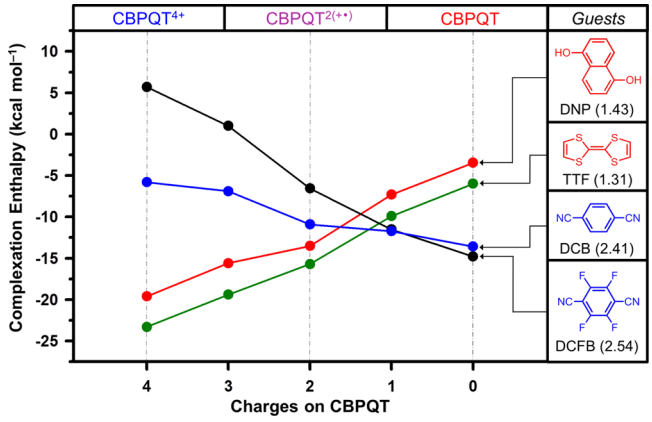

Figure 8. Plot of the complexation enthalpies derived from density functional theory calculations between the cyclophane in different oxidation states and DNP, TTF, DCB and DCFB with the calculated Mulliken electronegativities indicated in parentheses. The complexation enthalpy is defined as the energy it takes for a guest to replace two MeCN molecules originally sitting in the cavity of the cyclophane (representing the neutral CBPQT in MeCN solvent) to form a 1:1 inclusion complex with the guest.

DOI: 10.1021/jacs.5b05618
J. Am. Chem. Soc. 2015, 137, 11057−11068

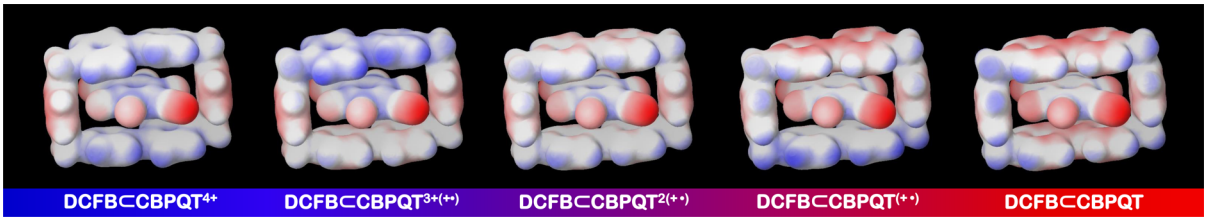

Figure 9. Electrostatic potential map in space-filling formula of the inclusion complex between DCFB and the cyclophane in different oxidation states, from tetracationic $CBPQT^{4+}$ (left) to neutral CBPQT (right) including the intermediates radical cationic species in between. The color from red to blue indicates the change in electrostatic potential from negative to positive values. The white background has a different reference potential in each charge state as consequence of the different charge of the cyclophanes.

can be quantified (Figure 8) by their Mulliken electronegativities (MEN), defined[46] as the sum of their ionization energies and electron affinities and scaled to approach Pauling's definition of electronegativity. In the tetracationic state the complexation enthalpy increases with the electron-donating properties of the guest since the formation of the complexes under these conditions is based primarily on aromatic donor−acceptor interactions. This principle is demonstrated by the difference in binding energies of TTF and DNP (MEN values for TTF and DNP are 1.31 and 1.43, respectively), two well-known electron-rich guests of the $CBPQT^{4+}$ that afford complexation enthalpies of −23.3 and −19.6 kcal mol^{-1}, respectively. The relatively high affinity of the fully charged cyclophane for electron-rich guests decreases significantly on altering the redox state of the ring to the dicationic and neutral forms as a result of the loss of the CT interactions. The rapid dissociation of the complex between the DNP and the ring, after its reduction to the diradical dicationic state, as a consequence of the attenuation of the donor−acceptor interactions has been demonstrated[47] experimentally previously. For electron-poor guests, such as DCB (MEN = 2.41) and DCFB (MEN = 2.54), the opposite trend of the complexation enthalpies as functions of the redox states of the ring is observed. The DCB⊂CBPQT inclusion complex is 7.8 kcal mol^{-1} more stable than the one calculated for the ring in the tetracationic state. For the more electron-poor guest, DCFB, this reverse trend in complexation enthalpy reaches 20.5 kcal mol^{-1}. The electrostatic potential map for the inclusion complexes of the host with DCFB shows (Figure 9) that, once the reduction of the ring reaches its neutral state, the negative electrostatic potential (colored in red) is observed on the BIPY units of the CBPQT and on the electron-withdrawing substituents (−F and −C≡N) of the guest molecule. When the cyclophane is oxidized, the BIPY units (colored in blue) become relatively more positive.

3. CONCLUSION

We have shown that the cyclophane's affinity for guests can be switched from preferring π-electron-rich to π-electron-poor by simply altering the redox state of the electron-poor $CBPQT^{4+}$ ring to that of electron-rich CBPQT. Moreover, we demonstrated that it is possible to isolate the neutral CBPQT in solution as well as in the solid state. We have characterized this neutral state and probed its properties by (i) UV−vis, EPR, and NMR spectroscopies, (ii) single-crystal X-ray diffraction analyses, and (iii) quantum mechanics calculations. We have demonstrated the distinctive properties emerging from the reduction of $CBPQT^{4+}$ to its neutral form by testing its ability to form inclusion complexes with electron-poor guests such 1,4-dicyanobenzene or 1,4-dicyanotetrafluorobenzene.

This appreciation of the binding capabilities of this neutral host is the first step toward its use in the template-directed synthesis of exotic MIMs that, thanks to the unique electronic properties of neutral CBPQT, are more than likely to display novel properties. Indeed, the translation of the protocol for the isolation of fully reduced CBPQT to the existing donor−acceptor catenanes and rotaxanes, comprising the $CBPQT^{4+}$ ring, now seems a distinct possibility. This opportunity of controlling the properties of MIMs by reducing the $CBPQT^{4+}$ ring to its neutral state, followed by the isolation of a range of new catenanes and rotaxanes will allow the properties of these neutral MIMs to be investigated from a totally different perspective.

The quantum mechanical description of the energy levels associated with the formation of the inclusion complexes supports this vision. Our investigations demonstrate a change in the nature of the binding mode that is dependent on the oxidation state of the cyclophane, leading to dominant interactions that range from being aromatic donor−acceptor in the case of the tetracationic $CBPQT^{4+}$ ring to being electrostatic when the cyclophane is fully reduced.

Another noteworthy feature of the neutral CBPQT host is its low reduction potential. Its propensity to undergo rapid electron transfer, together with its ability to form 1:1 inclusion complexes with electron-poor guests, could have important implications for the use of the neutral CBPQT as a catalyst for reduction processes in biphasic environments. Furthermore, the electronic properties of these neutral compounds and their 1:1 inclusion complexes could allow them to serve as alternative supramolecular systems for integration into devices capable of solid-state conductivity.

■ ASSOCIATED CONTENT

Supporting Information

The Supporting Information is available free of charge on the ACS Publications website at DOI: 10.1021/jacs.5b05618.

Full details of instrumentation and analytical techniques; detailed NMR spectroscopic investigations of CBPQT; UV−vis and EPR spectroscopic data; atomic coordinates and energies for all species in computational studies (PDF)

X-ray crystallographic analysis data for CBPQT (CIF)

X-ray crystallographic analysis data for MS (CIF)

X-ray crystallographic analysis data for (CBPQT)-($CBPQT{\cdot}2PF_6$) (CIF)

X-ray crystallographic analysis data for DCB⊂CBPQT (CIF)

DOI: 10.1021/jacs.5b05618
J. Am. Chem. Soc. 2015, 137, 11057−11068

AUTHOR INFORMATION

Corresponding Author

*stoddart@northwestern.edu

Present Addresses

[⊥](M.F.) Istituto Italiano di Tecnologia, Via Morego 30, 16163 Genova, Italy

[#](G.B.) Department of Chemistry, University of California, Berkeley, California 94720-1460, USA

Notes

The authors declare no competing financial interest.

ACKNOWLEDGMENTS

We thank Dr. Amy Sarjeant and Charlotte C. Stern for solving the single-crystal X-ray structures. This research is part (Project 32-949) of the Joint Center of Excellence in Integrated Nano-Systems (JCIN) at King Abdulaziz City for Science and Technology (KACST) and Northwestern University (NU). The authors thank both KACST and NU for their continued support of this research. M.R.W. and S.M.D. acknowledge support from the National Science Foundation (NSF) under Grant No. CHE-1266201. W.G.L. and W.A.G. were supported by NSF-EFRI-ODISSEI 1332411. Y.W. thanks the Fulbright Scholar Program for a Research Fellowship and also acknowledges additional support from a Ryan Fellowship awarded under the auspices of the NU International Institute of Nanotechnology (IIN).

REFERENCES

(1) (a) Meyer, E. A.; Castellano, R. K.; Diederich, F. *Angew. Chem., Int. Ed.* **2003**, *42*, 1210−1250. (b) Goodey, N. M.; Benkovic, S. J. *Nat. Chem. Biol.* **2008**, *4*, 474−482. (c) Smock, R. G.; Gierasch, L. M. *Science* **2009**, *324*, 198−203.

(2) (a) Lehn, J.-M. *Science* **1985**, *227*, 849−856. (b) Beer, P. D.; Gale, P. A.; Smith, D. K. *Supramolecular Chemistry*; Oxford University Press: Oxford, U.K., 1999. (c) Hoeben, F. J. M.; Jonkheijm, P.; Meijer, E. W.; Schenning, A. P. H. J. *Chem. Rev.* **2005**, *105*, 1491−1546. (d) Steed, J. W.; Atwood, J. L. *Supramolecular Chemistry*; Wiley-VCH: Weinheim, Germany, 2009. (e) Safont-Sempere, M. M.; Fernández, G.; Würthner, F. *Chem. Rev.* **2011**, *111*, 5784−5814.

(3) Cyclodextrins: (a) Alston, D. R.; Slawin, A. M. Z.; Stoddart, J. F.; Williams, D. J.; Zarzycki, R. *Angew. Chem., Int. Ed. Engl.* **1988**, *27*, 1184−1185. (b) Wenz, G. *Angew. Chem., Int. Ed. Engl.* **1994**, *33*, 803−822. (c) Rekharsky, M. V.; Inoue, Y. *Chem. Rev.* **1998**, *98*, 1875−1918. (d) Craig, M. R.; Hutchings, M. G.; Claridge, T. D. W.; Anderson, H. L. *Angew. Chem., Int. Ed.* **2001**, *40*, 1071−1074. (e) Harada, A.; Takashima, Y.; Yamaguchi, H. *Chem. Soc. Rev.* **2009**, *38*, 875−882. (f) Harada, A.; Kobayashi, R.; Takashima, Y.; Hashidzume, A.; Yamaguchi, H. *Nat. Chem.* **2011**, *3*, 34−37. (g) Crini, G. *Chem. Rev.* **2014**, *114*, 10940−10975. (h) Yang, C.; Inoue, Y. *Chem. Soc. Rev.* **2014**, *43*, 4123−4143.

(4) Cucurbiturils: (a) Freeman, W. A.; Mock, W. L.; Shih, N.-Y. *J. Am. Chem. Soc.* **1981**, *103*, 7367−7368. (b) Kim, K. *Chem. Soc. Rev.* **2002**, *31*, 96−107. (c) Lagona, J.; Mukhopadhyay, P.; Chakrabarti, S.; Isaacs, L. *Angew. Chem., Int. Ed.* **2005**, *44*, 4844−4870. (d) Kim, K.; Selvapalam, N.; Ko, Y.-H.; Park, K.-M.; Kim, D.; Kim, J. *Chem. Soc. Rev.* **2007**, *36*, 267−279. (e) Gao, C.; Silvi, S.; Ma, X.; Tian, H.; Credi, A.; Venturi, M. *Chem. - Eur. J.* **2012**, *18*, 16911−16921. (f) Lee, T.-C.; Kalenius, E.; Lazar, A. I.; Assaf, K. I.; Kuhnert, N.; Grün, C. H.; Jänis, J.; Scherman, O. A.; Nau, W. M. *Nat. Chem.* **2013**, *5*, 376−382. (g) Isaacs, L. *Acc. Chem. Res.* **2014**, *47*, 2052−2062.

(5) Calixarenes: (a) Gutsche, C. D. *Acc. Chem. Res.* **1983**, *16*, 161−170. (b) Reinhoudt, D. N.; Dijkstra, P. J.; In't Veld, P. J. A.; Bugge, K. E.; Harkema, S.; Ungaro, R.; Ghidini, E. *J. Am. Chem. Soc.* **1987**, *109*, 4761−4762. (c) Gale, P. A.; Sessler, J. L.; Král, V.; Lynch, V. *J. Am. Chem. Soc.* **1996**, *118*, 5140−5141. (d) Ikeda, A.; Shinkai, S. *Chem. Rev.* **1997**, *97*, 1713−1734. (e) Bucher, C.; Zimmerman, R. S.; Lynch, V.; Král, V.; Sessler, J. L. *J. Am. Chem. Soc.* **2001**, *123*, 2099−2100. (f) Dalgarno, S. J.; Thallapally, P. K.; Barbour, L. J.; Atwood, J. L. *Chem. Soc. Rev.* **2007**, *36*, 236−245. (g) Bagnacani, V.; Franceschi, V.; Bassi, M.; Lomazzi, M.; Donofrio, G.; Sansone, F.; Casnati, A.; Ungaro, R. *Nat. Commun.* **2013**, *4*, 1721.

(6) Pillarenes: (a) Ogoshi, T.; Kanai, S.; Fujinami, S.; Yamagishi, T.-A.; Nakamoto, Y. *J. Am. Chem. Soc.* **2008**, *130*, 5022−5023. (b) Semeraro, M.; Arduini, A.; Baroncini, M.; Battelli, R.; Credi, A.; Venturi, M.; Pochini, A.; Secchi, A.; Silvi, S. *Chem. - Eur. J.* **2010**, *16*, 3467−3475. (c) Strutt, N. L.; Forgan, R. S.; Spruell, J. M.; Botros, Y. Y.; Stoddart, J. F. *J. Am. Chem. Soc.* **2011**, *133*, 5668−5671. (d) Cragg, P. J.; Sharma, K. *Chem. Soc. Rev.* **2012**, *41*, 597−607. (e) Ogoshi, T.; Shiga, R.; Yamagishi, T. *J. Am. Chem. Soc.* **2012**, *134*, 4577−4580. (f) Strutt, N. L.; Zhang, H.; Schneebeli, S. T.; Stoddart, J. F. *Acc. Chem. Res.* **2014**, *47*, 2631−2642.

(7) Imidazolium derivatives: (a) Yoon, J.; Kim, S. K.; Singh, N. J.; Kim, K. S. *Chem. Soc. Rev.* **2006**, *35*, 355−360. (b) Gong, H.-Y.; Rambo, B. M.; Karnas, E.; Lynch, V. M.; Sessler, J. L. *Nat. Chem.* **2010**, *2*, 406−409. (c) Serpell, C. J.; Cookson, J.; Thompson, A. L.; Beer, P. D. *Chem. Sci.* **2011**, *2*, 494−500. (d) Gong, H.-Y.; Rambo, B. M.; Lynch, V. M.; Keller, K. M.; Sessler, J. L. *Chem. - Eur. J.* **2012**, *18*, 7803−7809. (e) Rambo, B. M.; Gong, H. Y.; Oh, M.; Sessler, J. L. *Acc. Chem. Res.* **2012**, *45*, 1390−1401.

(8) Cyclophanes: (a) Diederich, F.; Dick, K. *Angew. Chem., Int. Ed. Engl.* **1983**, *22*, 715−716. (b) Bühner, M.; Geuder, W.; Gries, W.-K.; Hünig, S.; Koch, M.; Poll, T. *Angew. Chem., Int. Ed. Engl.* **1988**, *27*, 1553−1556. (c) Vögtle, F. *Cyclophane Chemistry*; Teubner: Stuttgart, 1990. (d) Ferguson, S. B.; Sanford, E. M.; Seward, E. M.; Diederich, F. *J. Am. Chem. Soc.* **1991**, *113*, 5410−5419. (e) Diederich, F. In *Modern Cyclophane Chemistry*; Gleiter, R., Hopf, H., Eds.; Wiley-VCH: Weinheim, 2005; pp 519−546.

(9) (a) Catenanes, Rotaxanes, and Knots. In *Organic Chemistry*; Schill, G., Ed.; Academic Press: New York, 1971; Vol. 22. (b) Dietrich-Buchecker, C. O.; Sauvage, J.-P. *Chem. Rev.* **1987**, *87*, 795−810. (c) Hunter, C. A. *J. Chem. Soc., Chem. Commun.* **1991**, 749−751. (d) Anderson, S.; Anderson, H. L.; Sanders, J. K. M. *Acc. Chem. Res.* **1993**, *26*, 469−475. (e) Fujita, M.; Ibukuro, H.; Hagihara, H.; Ogura, K. *Nature* **1994**, *367*, 720−723. (f) Amabilino, D. B.; Stoddart, J. F. *Chem. Rev.* **1995**, *95*, 2725−2828. (g) Yamamoto, C.; Okamoto, Y.; Schmidt, T.; Jäger, R.; Vögtle, F. *J. Am. Chem. Soc.* **1997**, *119*, 10547−10548. (h) Hamilton, D. G.; Feeder, N.; Prodi, L.; Teat, S. J.; Clegg, W.; Sanders, J. K. M. *J. Am. Chem. Soc.* **1998**, *120*, 1096−1097. (i) Dietrich-Buchecker, C.; Sauvage, J.-P. Molecular Catenanes, Rotaxanes and Knots. *A Journey Through the World of Molecular Topology*; Wiley-VCH: Weinheim, 1999. (j) Fujita, M. *Acc. Chem. Res.* **1999**, *32*, 53−61. (k) Harada, H. *Acc. Chem. Res.* **2001**, *34*, 456−464. (l) Chatterjee, M. N.; Kay, E. R.; Leigh, D. A. *J. Am. Chem. Soc.* **2006**, *128*, 4058−4073. (m) Faiz, J. A.; Heitz, V.; Sauvage, J.-P. *Chem. Soc. Rev.* **2009**, *38*, 422−442. (n) Stoddart, J. F. *Chem. Soc. Rev.* **2009**, *38*, 1802−1820. (o) Cao, D.; Amelia, M.; Klivansky, L. M.; Koshkakaryan, G.; Khan, S. I.; Semeraro, M.; Silvi, S.; Venturi, M.; Credi, A.; Liu, Y. *J. Am. Chem. Soc.* **2010**, *132*, 1110−1122. (p) Beves, J. E.; Blight, B. A.; Campbell, C. J.; Leigh, D. A.; McBurney, R. T. *Angew. Chem., Int. Ed.* **2011**, *50*, 9260−9327. (q) Spence, G. T.; Beer, P. D. *Acc. Chem. Res.* **2013**, *46*, 571−586. (r) Ayme, J.-F.; Beves, J. E.; Campbell, C. J.; Leigh, D. A. *Chem. Soc. Rev.* **2013**, *42*, 1700−1712.

(10) (a) Dietrich-Buchecker, C. O.; Sauvage, J.-P.; Kintzinger, J.-P. *Tetrahedron Lett.* **1983**, *24*, 5095−5098. (b) Bissell, R. A.; Cordova, E.; Kaifer, A. E.; Stoddart, J. F. *Nature* **1994**, *369*, 133−136. (c) Collin, J.-P.; Dietrich-Buchecker, C. O.; Jimenez-Molero, M. C.; Sauvage, J.-P. *Acc. Chem. Res.* **2001**, *34*, 477−487. (d) Kay, E. R.; Leigh, D. A.; Zerbetto, F. *Angew. Chem., Int. Ed.* **2007**, *46*, 72−191. (e) Balzani, V.; Venturi, M.; Credi, A. *Molecular Devices and Machines—Concepts and Perspectives for the Nanoworld*; Wiley-VCH: Weinheim, 2008. (f) Coskun, A.; Banaszak, M.; Astumian, R. D.; Stoddart, J. F.; Grzybowski, B. A. *Chem. Soc. Rev.* **2012**, *41*, 19−30.

(11) (a) Odell, B.; Reddington, M. V.; Slawin, A. M.; Spencer, N.; Stoddart, J. F.; Williams, D. J. *Angew. Chem., Int. Ed. Engl.* **1988**, *27*,

DOI: 10.1021/jacs.5b05618
J. Am. Chem. Soc. 2015, 137, 11057−11068

1547−1550. (b) Ashton, P. R.; Odell, B.; Reddington, M. V.; Slawin, A. M. Z.; Stoddart, J. F.; Williams, D. J. *Angew. Chem., Int. Ed. Engl.* **1988**, *27*, 1550−1553. (c) Ashton, P. R.; Brown, C. L.; Chrystal, E. J. T.; Goodnow, T. T.; Kaifer, A. E.; Parry, K. P.; Philp, D.; Slawin, A. M. Z.; Spencer, N.; Stoddart, J. F.; Williams, D. J. *J. Chem. Soc., Chem. Commun.* **1991**, 634−637. (d) Amabilino, D. B.; Stoddart, J. F. *Pure Appl. Chem.* **1993**, *65*, 2351−2359. (e) Anelli, P. L.; Spencer, N.; Stoddart, J. F. *J. Am. Chem. Soc.* **1991**, *113*, 5131−5135. (f) Asakawa, M.; Dehaen, W.; L'Abbe, G.; Menzer, S.; Nouwen, J.; Raymo, F. M.; Stoddart, J. F.; Williams, D. J. *J. Org. Chem.* **1996**, *61*, 9591−9595. (g) D'Acerno, C.; Doddi, G.; Ercolani, G.; Mencarelli, P. *Chem. - Eur. J.* **2000**, *6*, 3540−3546. (h) Tseng, H.-R.; Vignon, S. A.; Stoddart, J. F. *Angew. Chem., Int. Ed.* **2003**, *42*, 1491−1493. (i) Doddi, G.; Ercolani, G.; Mencarelli, P.; Piermattei, A. *J. Org. Chem.* **2005**, *70*, 3761−3764. (j) Koshkakaryan, G.; Cao, D.; Klivansky, L. M.; Teat, S. J.; Tran, J. L.; Liu, Y. *Org. Lett.* **2010**, *12*, 1528−1531. (k) Fahrenbach, A. C.; Bruns, C. J.; Cao, D.; Stoddart, J. F. *Acc. Chem. Res.* **2012**, *45*, 1581−1592.

(12) (a) Philp, D.; Slawin, A. M. Z.; Spencer, N.; Stoddart, J. F.; Williams, D. J. *J. Chem. Soc., Chem. Commun.* **1991**, *22*, 1584−1586. (b) Choi, J. W.; Flood, A. H.; Steuerman, D. W.; Nygaard, S.; Braunschweig, A. B.; Moonen, N. N. P.; Laursen, B. W.; Luo, Y.; DeIonno, E.; Peters, A. J.; Jeppesen, J. O.; Xu, K.; Stoddart, J. F.; Heath, J. R. *Chem. - Eur. J.* **2006**, *12*, 261−279. (c) Canevet, D.; Sallé, M.; Zhang, G.; Zhang, D.; Zhu, D. *Chem. Commun.* **2009**, *17*, 2245−2269. (d) Coskun, A.; Klajn, R.; Fang, L.; Olson, M. A.; Wesson, P. J.; Trabolsi, A.; Dey, S. K.; Grzybowski, B. A.; Stoddart, J. F. *J. Am. Chem. Soc.* **2010**, *132*, 4310−4320. (e) Hansen, S. W.; Stein, P. C.; Sørensen, A.; Share, A. I.; Witlicki, E. H.; Kongsted, J.; Flood, A. H.; Jeppesen, J. O. *J. Am. Chem. Soc.* **2012**, *134*, 3857−3863.

(13) Olson, M. A.; Botros, Y. Y.; Stoddart, J. F. *Pure Appl. Chem.* **2010**, *82*, 1569−1574.

(14) Coskun, A.; Spruell, J. M.; Barin, G.; Dichtel, W. R.; Flood, A. H.; Botros, Y. Y.; Stoddart, J. F. *Chem. Soc. Rev.* **2012**, *41*, 4827−4859.

(15) For an early example of constitutional isomers of $CBPQT^{4+}$, see: Amabilino, D. B.; Ashton, P. R.; Tolley, M. S.; Stoddart, J. F.; Williams, D. J. *Angew. Chem., Int. Ed. Engl.* **1993**, *32*, 1297−1303. For a chiral tetracationic cyclophane, see: Ashton, P. R.; Bravo, J. A.; Raymo, F. M.; Stoddart, J. F.; White, A. J. P.; Williams, D. J. *Eur. J. Org. Chem.* **1999**, *4*, 899−908.

(16) (a) Asakawa, M.; Ashton, P. R.; Menzer, S.; Raymo, F. M.; Stoddart, J. F. *Chem. - Eur. J.* **1996**, *2*, 877−893. (b) Ashton, P. R.; Menzer, S.; Raymo, F. M.; Shimizu, G. K. H.; Stoddart, J. F.; Williams, D. J. *Chem. Commun.* **1996**, 487−490. (c) Spruell, J. M.; Coskun, A.; Friedman, D. C.; Forgan, R. S.; Sarjeant, A. A.; Trabolsi, A.; Fahrenbach, A. C.; Barin, G.; Paxton, W. F.; Dey, S. K.; Olson, M. A.; Benítez, D.; Tkatchouk, E.; Colvin, M. T.; Carmielli, R.; Caldwell, S. T.; Rosair, G. M.; Gunatilaka Hewage, S.; Duclairoir, F.; Seymour, J. L.; Slawin, A. M. Z.; Goddard, W. A., III; Wasielewski, M. R.; Cooke, G.; Stoddart, J. F. *Nat. Chem.* **2010**, *2*, 870−879. (d) Barin, B.; Frasconi, M.; Dyar, S. M.; Iehl, J.; Buyukcakir, O.; Sarjeant, A. A.; Carmieli, R.; Coskun, A.; Wasielewski, M. R.; Stoddart, J. F. *J. Am. Chem. Soc.* **2013**, *135*, 2466−2469.

(17) (a) Barnes, J. C.; Juríček, M.; Strutt, N. L.; Frasconi, M.; Sampath, S.; Giesener, M. A.; McGrier, P. L.; Bruns, C. J.; Stern, C. L.; Sarjeant, A. A.; Stoddart, J. F. *J. Am. Chem. Soc.* **2013**, *135*, 183−192. (b) Bachrach, S. M. *J. Phys. Chem. A* **2013**, *117*, 8484−8491. (c) Young, R. M.; Dyar, S. M.; Barnes, J. C.; Juríček, M.; Stoddart, J. F.; Co, D. T.; Wasielewski, M. R. *J. Phys. Chem. A* **2013**, *117*, 12438−12448. (d) Juríček, M.; Strutt, N. L.; Barnes, J. C.; Butterfield, A. M.; Dale, E. J.; Baldridge, K. K.; Stoddart, J. F.; Siegel, J. S. *Nat. Chem.* **2014**, *6*, 222−228. (e) Ryan, S. T. J.; Del Barrio, J.; Ghosh, I.; Biedermann, F.; Lazar, A. I.; Lan, Y.; Coulston, R. J.; Nau, W. N.; Scherman, O. A. *J. Am. Chem. Soc.* **2014**, *136*, 9053−9060.

(18) (a) Trabolsi, A.; Khashab, N.; Fahrenbach, A. C.; Friedman, D. C.; Colvin, M. T.; Cotí, K. K.; Benítez, D.; Tkatchouk, E.; Olsen, J.-C.; Belowich, M. E.; Carmielli, R.; Khatib, H. A.; Goddard, W. A., III; Wasielewski, M. R.; Stoddart, J. F. *Nat. Chem.* **2010**, *2*, 42−49. (b) Fahrenbach, A. C.; Barnes, J. C.; Lanfranchi, D. A.; Li, H.; Coskun, A.; Gassensmith, J. J.; Liu, Z.; Benítez, D.; Trabolsi, A.; Goddard, W. A., III; Elhabiri, M.; Stoddart, J. F. *J. Am. Chem. Soc.* **2012**, *134*, 3061−3072.

(19) (a) Li, H.; Zhu, Z.; Fahrenbach, A. C.; Cao, D.; Liu, W.-G.; Dey, S. K.; Basu, S.; Trabolsi, A.; Botros, Y. Y.; Goddard, W. A., III; Stoddart, J. F. *J. Am. Chem. Soc.* **2013**, *135*, 456−467. (b) Witus, L. S.; Hartlieb, K. J.; Wang, Y.; Prokofjevs, A.; Frasconi, M.; Barnes, J. C.; Dale, E. J.; Fahrenbach, A. C.; Stoddart, J. F. *Org. Biomol. Chem.* **2014**, *12*, 6089−6093. (c) Bruns, C. J.; Frasconi, M.; Iehl, J.; Hartlieb, K. J.; Schneebeli, S. T.; Cheng, C.; Stupp, S. I.; Stoddart, J. F. *J. Am. Chem. Soc.* **2014**, *136*, 4714−4723.

(20) Template-directed synthesis of a [2]rotaxane induced by radical-stabilized inclusion complexes of $CBPQT^{2(\bullet+)}$ ring encircling a dumbbell containing a $BIPY^{\bullet+}$ unit was achieved employing a threading followed by stoppering approach. The radical-cationic species, which promote the generation of the inclusion complex, were generated by the $[Ru\text{-}(bpy)_3]^{2+}$ reducing system (bpy = 2,2′-bipyridine). See: Li, H.; Fahrenbach, A. C.; Coskun, A.; Zhu, Z.; Barin, G.; Zhao, Y.-L.; Botros, Y. Y.; Sauvage, J.-P.; Stoddart, J. F. *Angew. Chem., Int. Ed.* **2011**, *50*, 6782−6788. A chemical reducing agent, Zn dust, was employed to obtain radical cationic $BIPY^{\bullet+}$ derivatives involved in the formation of inclusion complexes for the radical-templated synthesis of a homologous series of [2]rotaxanes. See: Li, H.; Zhu, Z.; Fahrenbach, A. C.; Savoie, B. M.; Ke, C.; Barnes, J. C.; Lei, J.; Zhao, Y.-L.; Lilley, L. M.; Marks, T. J.; Ratner, M. A.; Stoddart, J. F. *J. Am. Chem. Soc.* **2013**, *135*, 456−467.

(21) (a) Barnes, J. C.; Fahrenbach, A. C.; Cao, D.; Dyar, S. M.; Frasconi, M.; Giesener, M. A.; Benítez, D.; Tkatchouk, E.; Chernyashevskyy, O.; Shin, W. H.; Li, H.; Sampath, S.; Stern, C. L.; Sarjeant, A. A.; Hartlieb, K. J.; Liu, Z.; Carmieli, R.; Botros, Y. Y.; Choi, J. W.; Slawin, A. M. Z.; Ketterson, J. B.; Wasielewski, M. R.; Goddard, W. A., III; Stoddart, J. F. *Science* **2013**, *339*, 429−433. (b) Barnes, J. C.; Frasconi, M.; Young, R. M.; Khdary, N. H.; Liu, W.-G.; Dyar, S. M.; McGonigal, P. R.; Gibbs-Hall, I. C.; Diercks, C. S.; Sarjeant, A. A.; Stern, C. L.; Goddard, W. A., III; Wasielewski, M. R.; Stoddart, J. F. *J. Am. Chem. Soc.* **2014**, *136*, 10569−10572.

(22) (a) Carey, J. G.; Cairns, J. F.; Colchester, J. E. *J. Chem. Soc. D* **1969**, 1280−1281. (b) Mohammad. *J. Org. Chem.* **1987**, *52*, 2779−2782. (c) Monk, P. M. S. *The Viologens: Physicochemical Properties, Synthesis and Applications of the Salts of 4,4′-Bipyridine*; Wiley: New York, 1998. (d) Makarov, S. V.; Kudrik, E. V.; van Eldik, R.; Naidenko, E. V. *J. Chem. Soc., Dalton Trans.* **2002**, 4074−4076.

(23) For X-ray crystallographic analysis of methyl viologen in the fully reduced form, see: Bockman, T. M.; Kochi, J. K. *J. Org. Chem.* **1990**, *55*, 4127−4135.

(24) Derivatives of the dihydrobipyridine have been employed in electron-transfer reactions as redox mediators in a two-phase system. The photoreduction of the dicationic $BIPY^{2+}$ by $[Ru\text{-}(bpy)_3]^{2+}$ in an aqueous phase results in extraction into the organic layer of the radical cationic $BIPY^{\bullet+}$ species which undergoes disproportionation, generating the dicationic $BIPY^{2+}$, which returns to the aqueous layer, and neutral BIPY, which is capable of effecting a reductive dehalogenation reaction in the organic phase. See: (a) Goren, Z.; Willner, I. *J. Am. Chem. Soc.* **1983**, *105*, 7764−7767. (b) Maidan, R.; Goren, Z.; Becker, J. Y.; Willner, I. *J. Am. Chem. Soc.* **1984**, *106*, 6217−6222. (c) Maidan, R.; Willner, I. *J. Am. Chem. Soc.* **1986**, *108*, 1080−1082.

(25) Electrical conductivity measurements have been performed for neutral phenyl viologen. See: Porter, W. W., III; Vaid, T. P. *J. Org. Chem.* **2005**, *70*, 5028−5035. These studies conclude that the higher conductivity observed for the phenyl viologen in the neutral form, in comparison with the radical cationic state, can be explained in term of differences in geometrical relaxation during the hole transfer.

(26) Improved hole transport of electronic devices has been achieved by using viologen derivatives in the neutral state as functional components. See: (a) Porter, W. W., III; Vaid, T. P.; Rheingold, A. L. *J. Am. Chem. Soc.* **2005**, *127*, 16559−16566. (b) Kim, S. M.; Jang, J. H.; Kim, K. K.; Park, H. K.; Bae, J. J.; Yu, W. J.; Lee, I. H.; Kim, G.; Loc, D. D.; Kim, U. J.; Lee, E.-H.; Shin, H.-J.; Choi, J.-Y.; Lee, Y. H. *J. Am. Chem. Soc.* **2009**, *131*, 327−331. (c) Kiriya, D.; Tosun, M.; Zhao, P.; Kang, J. S.; Javey, A. *J. Am. Chem. Soc.* **2014**, *136*, 7853−7856. Layers

DOI: 10.1021/jacs.5b05618
J. Am. Chem. Soc. 2015, 137, 11057−11068

of neutral viologen doped with cobaltocene have been employed in inverted polymer solar cells as effective electron transport layers. See: (d) Kim, C. S.; Lee, S.; Tinker, L. L.; Bernhard, S.; Loo, Y.-L. *Chem. Mater.* **2009**, *21*, 4583−4588.

(27) (a) Kelly, T. R.; De Silva, H.; Silva, R. A. *Nature* **1999**, *401*, 150−154. (b) Kottas, G. S.; Clarke, L. I.; Horinek, D.; Michl, J. *Chem. Rev.* **2005**, *105*, 1281−1376. (c) Fletcher, S. P.; Dumur, F.; Pollard, M. M.; Feringa, B. L. *Science* **2005**, *310*, 80−84. (d) Perera, U. G. E.; Ample, E. F.; Kersell, H.; Zhang, Y.; Vives, G.; Echeverria, J.; Grisolia, M.; Rapenne, G.; Joachim, C.; Hla, S.-W. *Nat. Nanotechnol.* **2012**, *8*, 46−51. (e) Pospíšil, L.; Bednárová, L.; Štěpánek, L.; Slavíček, P.; Vávra, J.; Hromadová, M.; Dlouhá, H.; Tarábek, J.; Teplý, F. *J. Am. Chem. Soc.* **2014**, *136*, 10826−10829.

(28) The couple $CoCp_2^+/CoCp_2$ displays a formal potential ($E_{1/2}$) of −0.89 V vs SCE in MeCN. See: (a) Connelly, N. G.; Geiger, W. E. *Chem. Rev.* **1996**, *96*, 877−910. Cobaltocene has been employed as a one-electron reducing agent in the redox titration of viologen derivatives. See: (b) Funston, A.; Kirby, J. P.; Miller, J. R.; Pospíšil, L.; Fiedler, J.; Hromadová, M.; Gál, M.; Pecka, J.; Valášek, M.; Zawada, Z.; Rempala, P.; Michl, J. *J. Phys. Chem. A* **2005**, *109*, 10862−10869.

(29) The pH-dependent redox equilibria between methyl viologen and dithionite indicates that the kinetics of reduction of MV^{2+} to neutral MV proceeds at a significant rate around pH 9.0 or higher. See: Mayhew, S. G. *Eur. J. Biochem.* **1978**, *85*, 535−547. ^{1}H NMR spectra of an alkaline aqueous solution of $CBPQT^{4+}$ at pH 9.0 (CO_3^{2-}/HCO_3^-) display the characteristic chemical shift of the protons of $CBPQT^{4+}$ in D_2O, confirming the stability of the cyclophane in the experimental conditions employed for its reduction in the two-phase system. See the Supporting Information.

(30) The concentration of the CBPQT extracted into the organic phase was estimated using the extinction coefficient at 395 nm (ε = 45 000 M^{-1} cm^{-1}) reported for neutral viologen derivative. See: Watanabe, T.; Honda, K. *J. Phys. Chem.* **1982**, *86*, 2617−2619.

(31) NMR data for CBPQT. ^{1}H NMR (500 MHz, $C_6D_5CD_3$, 298 K): δ_H 7.15 (s, 8H, H_{xy}), 5.38−5.34 (m, 8H, H_β), 5.33−5.30 (m, 8H, H_α), 3.62 (s, 8H, H_{CH2}). ^{13}C NMR (125 MHz, $C_6D_5CD_3$, 298 K): δ_C 138.9 (C_z), 129.3 (C_α), 127.3 (C_{xy}), 109.9 (C_γ), 109.4 (C_β), 56.3 (C_C). Assignments of the resonances have been confirmed with the assistance of data from 2D NMR experiments. See the Supporting Information.

(32) Sue, C.-H.; Basu, S.; Fahrenbach, A. C.; Shveyd, A. K.; Dey, S. K.; Botros, Y. Y.; Stoddart, J. F. *Chem. Sci.* **2010**, *1*, 119−125.

(33) Single-crystal X-ray data were collected at 100 K on a Bruker Kappa APEX CCD diffractometer equipped with a Cu Kα microsource with Quazar optics. Crystallographic data for the structures reported in this article have been deposited with the Cambridge Crystallographic Data Center (CCDC) and can be obtained free of charge via www.ccdc.cam.ac.uk/data_request/cif.

(34) Crystal data for CBPQT. $3(C_{36}H_{32}N_4)\cdot 7(CH_3CN)$, M = 1849.34, trigonal, space group $R\bar{3}$ (No. 148), a = 22.3679(12) Å, c = 17.9046(10) Å, V = 7757.9(9) Å^3, T = 99.99 K, Z = 3, μ(Cu Kα) = 0.554 mm^{-1}. A total of 40 341 reflections were collected, of which 3124 were unique. Final $wR(F_2)$ = 0.0946. CCDC no. 985863.

(35) The relevant species for conduction by neutral violegen derivatives in the solid state is the radical cation. In contrast, the relevant species for the conduction of the radical cationic $BIPY^{\bullet+}$ in the solid state is the dicationic form; therefore, a significant geometrical change occurs during the hole transfer of radical cationic $BIPY^{\bullet+}$ in the solid state. For a survey on conductive properties of radical materials, see: Ratera, I.; Veciana, J. *Chem. Soc. Rev.* **2012**, *41*, 303−349.

(36) (a) Rosseinsky, D. R.; Monk, P. M. S. *J. Chem. Soc., Faraday Trans.* **1994**, *90*, 1127−1131. (b) Leblanc, N.; Mercier, N.; Toma, Q.; Kassiba, A. H.; Zorina, L.; Auban-Senzier, P.; Pasquier, C. *Chem. Commun.* **2013**, *49*, 10272−10274.

(37) Crystal data for $(CBPQT)(CBPQT\cdot 2PF_6)$. $(C_{36}H_{32}N_4)\cdot 2(PF_6)$, M = 665.62, monoclinic, space group $P2_1/m$ (No. 11), a = 9.9084(4) Å, b = 26.6982(9) Å, β = 99.632(2)°, V = 4129.1(3) Å^3, T = 99.99 K, Z = 4, μ(Cu Kα) = 1.048 mm^{-1}. A total of 6777 reflections were collected, of which 6766 were unique. Final $wR(F_2)$ = 0.2768. CCDC no. 985865.

(38) Some disorder is observed in the $(CBPQT)(CBPQT\cdot 2PF_6)$ structure in the rings comprising the one-dimensional channel, which are considered neutral CBPQT rings in the fully reduced state. The disorder can be ascribed to the fast electron exchange between the adjacent BIPY units of the cyclophane in different layers of the superstructure.

(39) The redox titration of MS^{4+} with $CoCp_2$ was performed in DMF solution on account of the low solubility of the fully reduced macrocycle in MeCN, even at very low concentrations.

(40) Crystal data for MS. $(C_{48}H_{40}N_4)$, M = 672.84, monoclinic, space group $P2_1/n$ (No. 14), a = 5.7756(3) Å, c = 14.5753(12) Å, β = 95.626(6)°, V = 1956.4(2) Å^3, T = 100.01 K, Z = 2, μ(Cu Kα) = 0.515 mm^{-1}. A total of 10 353 reflections were collected, of which 2041 were unique. Final $wR(F_2)$ = 0.2101. CCDC no. 985864.

(41) The fact that the shift of the resonances associated with the protons of the CBPQT host arises as consequence of the inclusion of the guest molecules within the cavity of the CBPQT is also supported by a control experiment performed on neutral methyl viologen as reference compound. The resonances associated with the protons of a $C_6D_5CD_3$ solution of neutral MV did not show any measurable shifts of their ^{1}H NMR resonances upon titration with DCB or DCFB. The small changes in chemical shifts obtained during ^{1}H NMR titrations between the CBPQT host and either DCB or DCFB as guests suggest, however, that the association constants (K_a values) between the neutral host and these electron deficient guests are so small in $C_6D_5CD_3$ solutions that it is not easy to obtain reliable estimates of the K_a values for their 1:1 complexes.

(42) (a) Kyba, E. P.; Helgeson, R. C.; Madan, K.; Gokel, G. W.; Tarnowski, T. L.; Moore, S. S.; Cram, D. D. *J. Am. Chem. Soc.* **1977**, *99*, 2564−2571. (b) Timko, J. M.; Moore, S. S.; Walba, D. M.; Hiberty, P. C.; Cram, D. D. *J. Am. Chem. Soc.* **1977**, *99*, 4207−4219.

(43) For seminal work on the classical notion of the interaction between aromatic rings, commonly referred to by the term π-staking, see: (a) Hunter, C. A.; Sanders, J. K. M. *J. Am. Chem. Soc.* **1990**, *112*, 5525−5534. (b) Cozzi, F.; Ponzini, F.; Annunziata, R.; Cinquini, M.; Siegel, J. *Angew. Chem., Int. Ed. Engl.* **1995**, *34*, 1019−1020. Recent studies on interactions between aromatic rings have revealed that solvation and desolvation effects can play a key role in determining the geometries and energetics of association, particularly in strongly interacting solvents. See: (c) Cubberley, M.; Iverson, B. *J. Am. Chem. Soc.* **2001**, *123*, 7560−7563. (d) Wheeler, S.; Houk, K. *J. Am. Chem. Soc.* **2008**, *130*, 10854−10855. (e) Martinez, C. R.; Iverson, B. L. *Chem. Sci.* **2012**, *3*, 2191−2201.

(44) Crystal data for $(DCB\subset CBPQT)$. $(C_8H_4N_2\subset C_{36}H_{32}N_4)$, M = 662.47, trigonal, space group $R\bar{3}$ (No. 148), a = 22.2705(9) Å, c = 17.9544(7) Å, V = 7711.9(7) Å^3, T = 99.99 K, Z = 9, μ(Cu Kα) = 0.599 mm^{-1}. A total of 16 258 reflections were collected, of which 2933 were unique. Final $wR(F_2)$ = 0.0803. CCDC no. 985862.

(45) Tannor, D. J.; Marten, B.; Murphy, R.; Friesner, R. A.; Sitkoff, D.; Nicholls, A.; Ringnalda, M.; Goddard, W. A., III; Honig, B. *J. Am. Chem. Soc.* **1994**, *116*, 11875−11882.

(46) For the definition and quantification of the Mulliken electronegativity refer to http://en.wikipedia.org/wiki/Electronegativity#Mulliken_electronegativity.

(47) (a) Ashton, P. R.; Ballardini, R.; Balzani, V.; Boyd, S. E.; Credi, A.; Gandolfi, M. T.; Gómez-López, M.; Iqbal, S.; Philp, D.; Preece, J. A.; Prodi, L.; Ricketts, H. G.; Stoddart, J. F.; Tolley, M. S.; Venturi, M.; White, A. J. P.; Williams, D. J. *Chem. - Eur. J.* **1997**, *3*, 152−165. (b) Scarpantonio, L.; Tron, A.; Destribats, C.; Godard, P.; McClenaghan, N. D. *Chem. Commun.* **2012**, *48*, 3981−3983. (c) Li, H.; Cheng, C. Y.; McGonigal, P. R.; Fahrenbach, A. C.; Frasconi, M.; Liu, W. G.; Zhu, Z. X.; Zhao, Y. L.; Ke, C. F.; Lei, J. Y.; Young, R. M.; Dyar, S. M.; Co, D. T.; Yang, Y. W.; Botros, Y. Y.; Goddard, W. A., III; Wasielewski, M. R.; Astumian, R. D.; Stoddart, J. F. *J. Am. Chem. Soc.* **2013**, *135*, 18609−18620.

DOI: 10.1021/jacs.5b05618
J. Am. Chem. Soc. 2015, 137, 11057−11068